An Improved Method to Detect Damage using Modal Strain Energy Based Damage Index

Wahalthantri B.L.*[1], Thambiratnam D.P.*, Chan T.H.T.*, Fawzia S.*

*School of Urban Development, Faculty of Built Environment and Engineering, Queensland University of Technology, Brisbane, Australia

Abstract:

This paper presents two novel concepts to enhance the accuracy of damage detection using the Modal Strain Energy based Damage Index (MSEDI) with the presence of noise in the mode shape data. Firstly, the paper presents a sequential curve fitting technique that reduces the effect of noise on the calculation process of the MSEDI, more effectively than the two commonly used curve fitting techniques; namely, polynomial and Fourier's series. Secondly, a probability based Generalized Damage Localization Index (GDLI) is proposed as a viable improvement to the damage detection process. The study uses a validated ABAQUS finite-element model of a reinforced concrete beam to obtain mode shape data in the undamaged and damaged states. Noise is simulated by adding three levels of random noise (1%, 3%, and 5%) to the mode shape data. Results show that damage detection is enhanced with increased number of modes and samples used with the GDLI.

Key Words: Modal strain energy based damage index, noise, sequential curve fitting technique, false alarms, probability, generalized damage localization index.

[1] Email: buddhi.wahalathantri@student.qut.edu.au , Tel: (+61)430649620 , Fax:+61 7 3138 1170

1. Introduction

Vibration Based Damage Identification Techniques (VBDITs) have achieved significant research interest in recent years, mainly due to their non-destructive nature, ability to provide uninterrupted use and their ability to detect inaccessible and invisible damage locations. The damage index method is one of the simplest approaches among the VBDITs presented in the literature and uses changes in vibration properties as parameters to detect damage. Many of the initial research on VBDITs attempted to detect damage using basic vibration parameters; namely, frequencies, mode shapes and damping values (Doebling et al. 1996, Salawu 1997 and Curadelli 2008). However, secondary damage indices derived using combinations and/or derivatives of basic vibration properties, have indicated better damage detection ability. The four most common secondary damage indices used in past research are based on changes in flexibility values, flexibility curvatures, mode shape derivatives and modal strain energy values (Doebling et al. 1996 and Alvandi and Cremona 2005). Alvandi and Cremona (2005) compared the damage detection ability of these four secondary damage indices under different noise levels. Following the pioneer work carried out by Mazurek (1997) and Doebling and Farrar (1998) on statistical significance of the damage detection process, Alvandi and Cremona (2005) used two probability based parameters (i.e. 1. probabilities of false alarms, and 2. probabilities of correct condition detection), to evaluate the four secondary damage indices mentioned above. Results of Alvandi and Cremona (2005) showed high stability of damage detection for the Modal Strain Energy based Damage Index (MSEDI) compared to the other three damage indices (changes in mode shape curvatures, flexibility values, and flexibility curvatures). However, their results indicated increased number of false alarms with increased noise levels in the mode shape data. Similar findings were reported by Shi and Law (1998).

Even though, previous research had signified the reduction of damage detection ability of the MSEDI in the presence of noise in mode shape data, no methods had been proposed to minimize the effects of noise. This study, therefore, examines the factors affecting the accuracy of the MSEDI and presents

two novel concepts to improve the damage detection ability of the MSEDI. As shown in section 1.2 of this paper, the curve fitting technique has a significant effect on the damage detection results, especially if mode shape values are polluted with noise. The two commonly used curve fitting techniques namely polynomial and Fourier series, lead to an increase in the number of false alarms as indicated in section 4.1. This paper proposes a sequential curve fitting technique that minimizes the impact of noise on calculation of mode shape curvatures and the subsequent calculation steps of the MSEDI. Secondly, the paper proposes a new damage index called the Generalized Damage Localization Index (GDLI) based on the probabilities of condition detection results of the MSEDI. The influence of higher modes and number of samples on the accuracy of the damage localization process is evaluated at the end of this paper.

The next section of the paper presents a brief literature review on the MSEDI and its use in damage detection. This is followed by a review of the computational steps associated with the MSEDI derivation process. Basic theory and equations are presented in section 2 of the paper. The method and results and discussion are presented in section 3 and section 4 respectively.

1.1.Modal Strain Energy Based Damage Index

Stubbs et al. (1992) pioneered the research on using changes in modal strain energy values to detect damage and proposed the first MSEDI for 1D elements. Stubbs et al. (1995) confirmed the applicability of the MSEDI, by detecting the damage in a steel bridge. Later, Cornwell et al. (1999) extended the above MSEDI for 2D structural elements such as plates. Since 1992, different formulae for MSEDIs have been presented by Stubbs et al. (1992), Cornwell et al. (1999), Park et al. (2002), Li et al. (2007), Shih et al. (2009) and Wahalathantri et al. (2010). Some other researchers who used the MSEDI to detect damage in structures are: Petro et al. 1997, Osegueda et al. 1997, Carrasco et al. 1997, Cornwell et al. 1998, Yoo et al. 1999, and Pereyra et al. 2000, and Alvandi and Cremona (2005).

Wahalathantri et al. (2010) proposed a weighting function that minimizes the intensity of false alarms

of the MSEDI at vicinities of nodal points (at points where the mode shape values become zero). In the present study, the concept of the weighting function as proposed by Wahalathantri et al. (2010) is combined with the MSEDI derived by Stubbs et al. (1992) to enhance damage detection. The necessary equations required to calculate the MSEDI are presented in section 2 of the paper.

1.2. Overview of the MSEDI calculation process

Computation of the MSEDI using displacement mode shapes involves three steps; namely, 1. calculating second derivatives of displacement mode shapes (mode shape curvatures), 2. integrating mode shape curvatures (to obtain strain energy values for individual elements and the whole structure), and 3. calculating the MSEDI (using equations given in section 2 of this paper). All three above steps are entirely based on computational techniques. Hence, the accuracy of the measurements is a key factor associated with the MSEDI. In particular, the processes leading to the calculation of mode shape curvatures should be improved as this paper does.

In most cases, mode shape curvatures are computed based on the displacement mode shapes using computational techniques such as the "central difference" formula (Salesh et al. 2004, Pandey et al. 1991). Chance et al. (1994) indicated that some false alarms are associated with the computational techniques when using the displacement mode shapes. Hence, Chance et al. (1994) proposed an alternative method to obtain mode shape curvatures using direct strain measurements. On the other hand, attempts have been made to use smoothing techniques such as the weighted residual penalty based technique to improve the calculation process involving displacement mode shapes (Maeck et al. 1999). The method proposed by Maeck et al. (1999) has drawbacks as the selection of the penalty factor is a trial-and-error process, which indicated problems of convergence if higher penalty factors are used. The method proposed in this paper uses three curve fitting techniques given in section 2.3 in a sequential order to minimise the effect of noise on subsequent calculation steps. Hence, the proposed curve fitting technique advances the use of displacement mode shapes for calculating the MSEDI.

2. Theory

2.1. MSEDI (Modal Strain Energy based Damage Index)

The modal strain energy, U_i of an Euler Bernoulli beam for the mode 'i' is given by Eqn.1, in which E, I, L, and φ_i represent the elastic modulus, second moment of area, length and the mode shape of the mode 'i' respectively. Eqn. 2 gives the elemental strain energy, U_{ij} of the element 'j'. (Alvandi and Cremona 2005, Shih et al. 2009).

The fractional strain energy, F_{ij}, of the element 'j' for the mode 'i' is defined as the strain energy of the element 'j' (U_{ij}) divided by the total strain energy (U_i) as given in Eqn. 3.

The first MSEDI of the element 'j' for the mode 'i' , $(\beta_{ij})_1$ as proposed by Stubbs et al (1992) is presented in Eqn. 4, in which subscripts 'd' and 'h' denote the damaged and undamaged states respectively

The damage index presented in Eqn. 4 and the weighting function, MF_i, proposed by Wahalathantri et al. (2010) are combined to form one of the MSEDI used in the present study as given in Eqn. 5. The MSEDI given in Eqn. 5 is calculated based on individual modes and denoted by β_{Aa} in which 'a' denotes the mode number, whereas 'A' serves the purpose of identification.

The weighting function MF_i is defined in Eqn. 6 in which, $[MSC]_{ij}$ denotes the mode shape curvature value at the centre of the element 'j' for mode 'i' and $|[MSC]_{ij}|_{max}$ denotes the absolute maximum value of the mode shape curvature of mode 'i'. (Wahalathantri et al. 2010)

The MSEDI derived by combining first 'b' modes is denoted by, β_{Bb}, and given in Eqn 7 in which 'B' serves the purpose of identification, while 'b' indicates that the damage index is derived using first 'b' modes (mode 1 to mode b). The 'MSV_i' term in Eqn. 7 denotes the modal sensitivity value of the mode 'i' as proposed by Lee et al. (2004), which assigns higher weight to the modes that are more sensitive to the damage. The MSV_i is defined in Eqn. 8 in which λ_i is the Eigen-value of the mode 'i'.

Where MSV_i is given as,

2.2. Computation of curvature of mode shapes using displacement mode shapes

As mentioned in the introduction section, this paper first examines the effect of the polynomial and Fourier series based curve fitting techniques on damage detection accuracy of the MSEDI. Two of the curve fitting techniques available in the MATLAB software (The Mathworks, Inc. 2010) are, therefore, used in the present study. These two curve fitting techniques are;

1. "spapi": Spline interpolation technique (curve fitting technique using polynomial function), and
2. Fourier series based curve fitting technique.

Order of these two curve fitting techniques should be determined from the number of available data points as described in section 2.3.1. The first curve fitting technique is denoted as CF01, whereas the second technique is denoted by CF02 in subsequent sections of the paper.

2.3. Proposed Sequential Curve Fitting Technique (CF03)

The new method proposed in this paper uses three curve fitting techniques available in the MATLAB software (The Mathworks, Inc. 2010) in a sequential order. In fact, the first ("csaps") and last ("spaps") curve fitting techniques are smoothing techniques. This sequential order is designed to minimise the effect of noise on subsequent calculation processes as confirmed by the results in section 4.1. Three curve fitting techniques combined in this paper in their sequential order are: 1. cubic smoothing spline technique ("csaps"), 2. Fourier series based technique, and 3. higher order smoothing spline technique ("spaps").

2.3.1. Minimum Requirements for CF03

As the proposed method, CF03, is based on curve fitting techniques available in the MATLAB software, the user should have access to the MATLAB software (The Mathworks, Inc., 2010) with the license for the curve fitting toolbox. The highest possible order (eight in this case) for both Fourier series and spline techniques ("spapi" or "spaps") are used. The orders of the curve fitting techniques are governed by the sampling resolution. The required minimum measurement points are tabulated in Table 1 for different orders of Fourier series. The order of the polynomial series used in two spline curve fitting techniques ("spapi" and "spaps") should be equal or less than the number of data points available. The cubic spline technique ("csaps") needs minimum of three data points.

In the present study, mode shape values at 20 nodes were extracted from the ABAQUS finite element simulation, and hence eighth order is used for both Fourier series and spline techniques in CF01, CF02 and CF03 as applicable.

2.4. Probability based Generalized Damage Localization Index (GDLI)

The probability values of the MSEDI indicate that higher the number of samples used, higher the accuracy of the damage detection results. This leads to the proposed GDLI given in Eqn. 9. The notation GDLI(β_{Cd}) is used to distinguish the MSEDI used when computing the GDLI (i.e. GDLI(β_{Cd}) = GDLI(β_{Aa}); if the MSEDI is calculated using individual modes, or GDLI(β_{Cd}) = GDLI(β_{Bb}); if the MSEDI is calculated by combining higher modes). The symbols α_j, α_m, and α_{sd} in Eqn. 9 represent the probability of detecting j^{th} element as a damaged element, mean value of α_j, and standard deviation of α_j respectively.

Any element with a positive value for the MSEDI (either β_{Aa} or β_{Bb}) is taken as a damaged element neglecting the value of the MSEDI. Hence, value of the generalized damage localization index does not account for damage severity but provides a comparative measure of the probability of being damaged.

3. Method

The main objective of this paper is to improve the damage detection results of the MSEDI with the presence of noise in the mode shape data. In order to achieve this, the following three enablers are required.

1. Studying the impact of curve fitting technique on accuracy of the damage detection process and verifying the improvement in damage detection with respect to the proposed sequential curve fitting technique,
2. Verifying the improved damage localization ability of the GDLI, and
3. Studying the influence of the number of samples and modes on damage detection process.

Figure 1 shows the methodology of this study including key steps in a schematic diagram. The overall analysis process relies on the vibration properties extracted from a validated ABAQUS finite element

model. The validation process is based on the reinforced concrete beam setup experimentally tested by Perera et al. (2008) and includes material model calibration using numerical technique proposed by Wahalathantri et al. (2011). The general arrangement of the four point beam bending test performed by Perera et al. (2008) and the cross section details of the beam are shown in Figure 2 and Figure 3 respectively. More details of finite element modelling and validation process are presented in sections 3.2 and 3.3 following the details of the experimental setup given in section 3.1. Section 3.4 provides details of the two case studies and methodology used in the analysis process.

3.1. Experiment Details

Perera et al. (2008) performed a comprehensive test on a reinforced concrete beam under four point bending test and presented both static and dynamic test results in terms of load vs. displacement curve, and first two frequency values. The tested RC beam was 4.54m in length with cross section dimensions of 0.32m and 0.22m in depth and width respectively. Figure 2 illustrates the loading arrangement with necessary dimensions whereas Figure 3 illustrates the cross section details of the RC beam including reinforcement details.

The elastic modulus, density and yield strength of reinforcement bars were taken as 210GPa, 7850kg/m^3 and 510MPa respectively. The experimentally measured compressive strength of concrete was 32MPa. Elastic modulus of concrete was calculated using linear portion of the load vs. displacement curve (Figure 4) presented by Perera et al. (2008).

3.2. Finite Element Modelling

The finite element package ABAQUS (Dassault Systèmes Simulia Corp. [SIMULIA] 2008) is used to simulate the load induced flexural cracking of a RC beam using modified material model presented by Wahalathantri et al. (2011). The main and shear reinforcement layers in the beam are simulated using smeared reinforcement layer technique (Abaqus Analysis User Manual – Abaqus Version 6.8 2008).

Three dimensional eight noded, fully integrated linear element type C3D8 is assigned for the concrete section. Four noded quadrilateral surface element type SFM3D4 is used for all the reinforcement layers, which are embedded in the concrete elements assuming full bond between reinforcement and concrete. Then validation of the finite element model is carried out using experiment test results of Perera et al. (2008).

3.3. Finite Element Model Validation

The experiment load vs. displacement curve given in Figure 4 is used to calibrate the material model required to develop the ABAQUS concrete damage plasticity model (Abaqus Analysis User Manual – Abaqus Version 6.8 2008) which accounts for tensile softening and stiffening. Stresses, inelastic strains and damage parameters obtained from the calibrated material model are given in Tables 2 and 3 for concrete under compression and tension respectively. The load vs. displacement curve obtained from ABAQUS finite element model is superposed in Figure 4, which indicates that the FEM validation is achieved under static condition for both linear and nonlinear regions.

Table 4 compares the frequency values between the present ABAQUS finite element model and the experimental results presented by Perera et al. (2008), under six different structural arrangements: 1. Undamaged beam, 2. Undamaged beam with two 100kg masses at 1.32m away from ends of the beam, 3. Undamaged beam with two 160kg masses at 1.32m away from ends of the beam, 4. Beam after load step of 8kN, 5. Beam after load step of 20kN (stage at damage initiation), and 6. Beam after load step of 52kN (at damaged state). The maximum percentage difference recorded in Table 4 is 2.56% and establishes the validation of the present ABAQUS finite element model under different structural arrangements including damage states.

3.4. Case Studies

This study is conducted using a simply supported reinforced concrete beam setup as shown in Figure

5. Cross section details and material properties used here are identical to that of the ABAQUS model described in the previous section. The self weight is applied as a uniformly distributed pressure over the top surface of the beam. Frequencies and mode shapes of the undamaged beam are obtained from the self loaded RC beam. The beam is then loaded at quarter span with a point load to simulate two levels of damage severity. A concentrated load (W) of 60kN is used to simulate a moderate damage severity whereas W=90kN is used to simulate higher damage severity. In both cases, frequencies and mode shapes are obtained for the first five flexural modes.

As vibration properties obtained from ABAQUS finite element models do not include measurement noise, all mode shapes are polluted with artificially generated random noise as used by other authors (Alvandi and Cremona 2005 and Shi and Law 1998). The polluted mode shape value at a general sampling point j can be given as in Eqn 10.

Where $(MS)_{jP}$ = Polluted mode shape value at sample point j, $(MS)_j$ = Mode shape value obtained from ABAQUS finite element model, Noise = Percentage of noise, $(RandVal)_j$ = randomly generated noise obtained from MATLAB function 'rand' (MATLAB® R2010b Help Browser 2010). For both damage cases, mode shape values are polluted with three noise levels (1%, 3%, and 5%).

A finer mesh with 60 elements along the longitudinal axis of the beam is used during the ABAQUS finite element simulation. However, mode shape values are only obtained at predefined 20 sampling points given in Figure 5 and processed through each of the three curve fitting techniques (CF01, CF02, and CF03). The unpolluted mode shape values are used to identify the baseline damage elements using MSEDI, β_{B5} (MSEDI derived by combining first five flexural modes using Eqn. 7). Polluted mode shape values are then used to calculate both forms of MSEDIs β_{Aa} (Eqn 5) for individual modes (subscript 'a' represents the mode number) and β_{Bb} (Eqn 7) for combinations of first five modes (subscript 'b' represents the number of modes combined).

The severe damage case (damage at W=90kN) is used to examine the accuracy of damage detection using each of the three curve fitting techniques (CF01, CF02, and CF03) under different noise levels. Results are evaluated based on the probability of correct condition detection and probability of false alarms using 10 samples for each noise level and curve fitting technique. The numbers of samples are varied to study their influence on the accuracy of the damage detection results. Three damage indices β_{A1}, β_{A2}, and β_{A3} are calculated to study the damage detection ability of first three modes on an individual basis. The damage indices β_{B2}, β_{B3}, and β_{B5} are calculated by combining first 2, 3 and 5 modes respectively to show the improvements in damage detection results when higher modes are included.

4. Results and Discussion

4.1. Evaluation of three curve fitting techniques

4.1.1. Evaluation Process

Damage detection abilities of three curve fitting techniques (CF01, CF02 and CF03) are first evaluated under three different noise levels (1%, 3%, and 5%) for the RC beam under severe damage level (at W=90kN). This leads to the evaluation of nine cases in total: CF01, CF02, and CF03, each with 1, 3 and 5% noise. For each of the nine evaluation cases, ten samples are used by polluting the mode shape values obtained from ABAQUS simulation with randomly generated noise as given in Eqn. 10 and hence a total of 90 samples are analysed during this stage.

Firstly, baseline damage elements are identified using the damage index β_{B5} (β_{Bb} with first five modes (b=5)) without adding any noise to the mode shape values. The damage identification using MSEDI β_{B5} is first compared with the smeared crack pattern (based on tensile damage parameter) observed in ABAQUS simulation (Figure 6). The observed ABAQUS smeared crack pattern (with a finer mesh having 60 elements in the longitudinal direction) is used to identify the damage states of 20 elements shown in Figure 5. The datum level to identify the damage using MSEDI β_{B5} is taken as zero as

Wahalathantri et al. (2010) proposed. It has to be noted that β_{B5} is a measure of change in strain energy values at two stages and hence value of β_{B5} can be positive or negative. The positive values are taken as an indication for the presence of damage, while the negative values are to be disregarded. On this basis, Figure 6 depicts that β_{B5} has correctly localized the vicinity of the severe damage region indicating that elements 4-10 are damaged. Therefore, baseline condition of elements 4-10 are taken as damaged whereas elements 1-3 and 11-20 are taken as undamaged.

Once the baseline conditions of elements are detected, β_{B5} values are re-calculated for all 90 samples. Positive values of β_{B5} are taken as damage indications for the candidate elements as did with the baseline condition detection process. The probability of damage indication (P_{dj}) and probability of undamaged indication (P_{uj}) for the j^{th} element is then calculated using Eqn 11 and Eqn 12 for each of the nine evaluation cases.

Eqn 11 and 12 are then used to calculate the probabilities of correct condition detection and probabilities of false alarms for the j^{th} element as defined below. The baseline condition of the element j is used as the comparative measure. (In all cases j represents the element number that varies from 1 to 20).

1. $P_{uuj} = P_{uj}$; if baseline condition of element j is indicated as undamaged (i.e. probability of correct condition detection of an undamaged element)
2. $P_{ddj} = P_{dj}$; if baseline condition of element j is indicated as damaged (i.e. probability of correct condition detection of a damaged element)
3. $P_{duj} = 1 - P_{uj}$; if baseline condition of element j is indicated as undamaged (i.e. probability of false alarm of detecting undamaged element as damaged)
4. $P_{udj} = 1 - P_{dj}$; if baseline condition of element j is indicated as damaged (i.e. probability of false

alarm of detecting damaged element as undamaged)

Eqn. 13-16 are used to derive another four parameters (A, B, C, and D) that are used to evaluate the overall performance of damage detection with respect to each of the curve fitting technique under three noise levels.

Parameters A and B represent the probabilities of correct condition detection whereas C and D indicate the probabilities of false alarms. Therefore, probability of correct condition detection and false alarms are respectively obtained from average of A and B and average of C and D respectively.

4.1.2. Results on evaluation of curve fitting techniques

Figure 7 represents probabilities for damage indication (P_{dj}) for three levels of noises for each of the three curve fitting techniques (CF01, CF02, and CF03). It can be seen that, both CF01 and CF02 caused a significant number of false alarms whereas CF03 has indicated lesser number of false alarms. CF03 has therefore detected the damage region more accurately compared to CF01 and CF02 under all three noise levels. However, the accuracy of damage detection has reduced with increased noise levels for all three curve fitting techniques.

The four parameters given in Eqn. 13-16 (A, B, C, and D) are used to present results in terms of probabilities of accurate condition detection and false alarms as tabulated in Table 5. With the

presence of 1% noise in measurements, percentage of accurate condition detection (average of A and B) for three curve fitting techniques are recorded as 78%, 76%, and 91% for CF01, CF02, and CF03 respectively. With increased noise levels, accuracy of correct condition detection is reduced to 59%, 55% and 91% for 3% noise and 59%, 57% and 86% for 5% noise for CF01, CF02, and CF03 respectively. CF01 and CF02 curve fitting techniques have indicated high percentages of false alarms with more than 20% false alarms at the lower noise level of 1% and more than 40% at moderate and higher noise levels of 3% and 5% respectively. The proposed sequential curve fitting technique (CF03) has recorded less than 10% false alarms at 1% and 3% noise levels and about 15% false alarms with the presence of 5% noise. These probability based values indicate the improvements achieved if the proposed sequential curve fitting technique is used in damage index calculation process. Only the proposed sequential curve fitting technique is therefore used in further studies reported in this paper.

4.2. Results on generalized damage localization index

Figure 8.a plots the variation of probability values of damage indication for all 20 elements which are calculated based on the MSEDI, β_{B5} using ten sample for severe damage level (at W=90kN) with 5% noise in mode shape values. These probability values produced five false alarms for the elements 1-3, 15 and 20. When the generalized damage localization index, GDLI(β_{B5}) is used in the damage detection process for this damage scenario with 5% noise, elements 3-10 are indicated as damage locations as shown in Figure 8.b. Compared to the baseline damage detection results in Figure 6, only one false alarm is recorded with GDLI(β_{B5}) (Figure 8.b) at element 3. At noise levels of 3% and 1%, no false alarms are recorded if GDLI(β_{B5}) is used in the damage detection process as illustrated in Figure 9.a and 9.b.

The GDLI is further evaluated for damage localization ability for the moderate damage severity (at W=60kN) with 5% noise in mode shapes. Baseline condition detection process using β_{B5} detects elements 4-9 are as damaged as shown in Figure 10. Compared to the intensity of β_{B5} for the severe

damage level (Figure 6), intensity of β_{B5} for the moderate damage level (Figure 10) has significantly reduced indicating the influence of damage severity on β_{B5} value.

Once baseline conditions of elements are detected, mode shape values are polluted to obtain 10 samples for each of the noise levels and GDLI(β_{B5}) is calculated. Figure 11 illustrates the damage identification results using GDLI(β_{B5}) for 5% noise for moderate damage level. Compared to the baseline detection results, presence of 5% noise in measurements has caused three false alarms corresponding to elements 1, 2 (detecting undamaged elements as damaged) and 4 (detecting damaged elements as undamaged). This implies that the accuracy of condition detection using GDLI is reduced with reduction in damage severity if the same number of samples is used. However, improved damage detection ability is recorded with the increased number of samples as shown in section 4.3.

4.3. Effect of number of samples

This section investigates the influence of the number of samples on the accuracy of the condition detection process using GDLI(β_{B5}) by varying the total number of samples to 5, 10, 15, 20, 25 and 30 for the moderate damage severity with 5% noise. Table 6 tabulates the element numbers corresponding to both positive false alarms (indication of undamaged elements as damaged) and negative false alarms (indication of damaged elements as undamaged). Table 6 indicates that significant numbers of false alarms are recorded if the sample number is equal or less than 15. With 20 samples, only one negative false alarm is recorded for the element 4. With 25 samples or above, no false alarms are recorded for the moderate damage severity with 5% noise. A minimum of 25 samples is therefore required to avoid all false alarms for the moderate damage severity with 5% noise.

Similar procedure is adopted to determine the minimum number of samples required (as given in Table 7) at lower noise levels for both damage severities. As Table 7 illustrates, the minimum numbers of samples are reduced to 20 and 15 at reduced noise levels of 3% and 1% respectively. Whereas for the severe damage case, minimum requirements are 15, 10 and 5 for 5%, 3% and 1% noise levels

respectively. These figures imply that the minimum number of samples required for correct condition detection depends on both the noise level and the damage severity. When GDLI is used to assess the state of a structure, the variation of the GDLI should therefore be tracked with the measurements taken.

4.4. Effect of higher modes

This section evaluates damage detection accuracy of GDLI using six forms of MSEDIs calculated using Eqn. 5 and Eqn. 7 for the moderate damage severity at 5% noise. Eqn. 5 is used to calculate β_{A1}, β_{A2}, and β_{A3} using first three individual modes. Eqn. 7 is used to calculate β_{B2}, β_{B3} and β_{B5} by combining first 2, 3 and 5 modes respectively. Six forms of GDLIs (GDLI(β_{A1}), GDLI(β_{A2}), GDLI(β_{A3}), GDLI (β_{B2}), GDLI (β_{B3}) and GDLI (β_{B5})) are then calculated using probabilities of damage indication using MSEDIs. Total number of samples used is set to 30, above the minimum requirements determined from Table 7.

First three GDLIs (GDLI(β_{A1}), GDLI(β_{A2}) and GDLI(β_{A3})) are used to study the accuracy of the condition detection results on individual mode basis. As Figure 13.a illustrates, GDLI(β_{A1}) indicates six positive false alarms for elements 1-3 and 18-20 with respect to the baseline condition of elements as detected from Figure 06. The GDLI(β_{A2}) in Figure 13.b gives 4 positive false alarms (elements 11-13, 19) and two negative false alarms (elements 4 and 9) whereas GDLI(β_{A3}) in Figure 13.c indicates four positive false alarms (elements 1-2, 10 and 15). Overall, generalized damage localization index derived using first three individual flexural modes does not accurately detect the condition of elements.

Three GDLIs derived by combining higher modes (GDLI(β_{B2}), GDLI(β_{B3}) and GDLI(β_{B5})) at 5% noise are illustrated in Figure 13.d - 13.f. Compared to Figure 13.a – 13.c, the number of false alarms are significantly reduced in Figure 13.d – 13.f, if higher modes are used in GDLI calculation process. GDLI(β_{B2}) in Figure 13.d has one positive false alarm for element 20 whereas GDLI(β_{B3}) in Figure 13.e has two negligible positive false alarms for elements 19 and 20. GDLI (β_{B5}) in Figure 13.f detects

the correct damage elements (elements 4-9) with no false alarms and hence provides the most accurate condition detection result proving the improved accuracy in damage detection with the addition of higher modes.

5. Significance and Conclusions

A detailed study on evaluating the effects of computational techniques on the MSEDI is presented in this paper. For the first time, problems associated with the simple curve fitting techniques are revealed indicating increased number of false alarms with increased noise level in the mode shape data. The proposed sequential curve fitting technique indicated a significant improvement in damage detection results by reducing the probabilities of false alarms. This method is based on three curve fitting techniques available in MATLAB software. As MATLAB or MATLAB supported software are widely used in most vibration data acquisition systems, the proposed method can be easily adopted into the damage detection process.

This paper also proposed a novel concept of a probability based generalized damage localization index (GDLI) which can be easily implemented on any of the continuous health monitoring systems. The improvements in damage detection results with respect to the GDLI are presented in this paper. Although, this paper was limited to examine improvement in damage detection using the GDLI in combination with MSEDI; the concept of the GDLI can be easily incorporated into other vibration based damage identification techniques.

Results in the paper show that the accuracy of the GDLI depends on damage severity, noise level, number of samples and modes. Higher noise levels and lower damage severity may indicate increased false alarms and hence may reduce the accuracy of the damage detection process. However, improved condition detection results can be obtained if the number of samples used in GDLI calculation is increased. In a continuous health monitoring system, GDLI can therefore be tracked with measurements taken to provide a reliable damage indication. This paper further demonstrates that

combination of higher modes in damage detection process using MSEDI provides improved condition detection results.

Acknowledgement

This paper forms part of a continuing study of structural health monitoring of structures conducted in Queensland University of Technology. B.L. Wahalathantri is supported by International Postgraduate Research Scholarship and Queensland University of Technology Postgraduate Research Award.

References

Abaqus Analysis User Manual – Abaqus Version 6.8. (2008). Retrieved May 5, 2011, from http://bee-pg-031941:2080 /v6.8/books/usb/default.htm

Alvandi, A. and Cremona, C. (2005). "Assessment of vibration-based damage identification techniques", *Journal of Sound and Vibration*, 292 , 179–202, 2005.

Carrasco, C., Osegueda, R., Ferregut, C. and Grygier, M. (1997). "Damage localization in a space truss model using modal strain energy", *Proceedings of International Modal Analysis Conference (IMAC-XV)*, Orlando, FL, 1786-1792, 1997.

Chance, J., Tomlinson, G.R., and Worden, K. (1994)."Simplified approach to the numerical and experimental modelling of the dynamics of a cracked beam", *Proceedings of International Modal Analysis Conference (IMAC-XII)*, 778, 1994.

Cornwell, P., Doebling, S.W. and Farrar, C.R. (1999). "Application of the strain energy damage detection method to plate-like structures", *Journal of Sound and Vibration*, 224 (2), 359 – 374, 1999.

Cornwell, P., Kam, M., Carlson, B., Hoerst, B., Doebling, S., and Farrar, C. (1998). "Comparative study of vibration-based damage ID algorithms", *Proceedings of International Modal Analysis Conference (IMAC-XVI)*, Santa Barbara, CA, 1710-1716, 1998.

Curadelli, R.O., Riera, J.D., Ambrosini, D. and Amani, M.G. (2008). "Damage detection by means of structural damping identification", *Engineering Structures*, 30, 3497-3504, 2008.

Dassault Systèmes Simulia Corp. [SIMULIA], 2008. Abaqus v. 6.8 [Software], Providence, RI: Dassault Systèmes Simulia Corp.

Doebling, S.W. and Farrar, C.F. (1998). "Statistical damage identification techniques applied to the I-40 bridge over the Rio Grande River", *Proceedings of the IMAC*, vol. 16, 1998, pp. 1717–1724.

Doebling, S.W., Farrar, C.R., Prime, M.B., and Shevit, D.W. (1996). "Damage identification and health monitoring of structural and mechanical systems from changes in their vibration characteristics: A literature review", *Los Alamos National Laboratory (LANL) Report No. LA-13070-MS*, 1996.

Lee, L.S., Karbhari, V.M., and Sikorsky, C. (2004). "Investigation of integrity and effectiveness of RC bridge deck rehabilitation with CFRP composites", *Final report submitted to the California Department of Transportation (Caltrans) under Contract No. 59A0249*, University of California, San Diego, California, 2004.

Li, J., Choi, F. C., Samali, B. and Crews, K. (2007)."Damage localization and severity evaluation of a beam-like timber structure based on modal strain energy and flexibility approaches", *Journal of Building Appraisal*, Vol. 2, No. 4, 323-334, 2007.

Maeck, J., AbdelWahab, M., and De Roec, G. (1999). "Damage localization in reinforced concrete beams by dynamic stiffness determination", *Proceedings of International Modal Analysis Conference (IMAC-XVII)*. Orlando, FL, 1289–95, 1999.

MATLAB® R2010b Help Browser, 2010. MATLAB® R2010b [Software], The MathWorks, Inc. 3 Apple Hill Drive Natick, MA 01760-2098

Mazurek, D.F. (1997). "Modal sensitivity to damage in multigirder bridges", *Proceedings of the IMAC*, vol. 15, 1997, pp. 1898–1982.

Osegueda, R.A., Carrasco, C.J., and Meza, A. (1997). “A modal strain energy distribution method to localize and quantify damage”, *Proceedings of International Modal Analysis Conference (IMAC-XV)*, Orlando, FL, 1298-1304, 1997.

Pandey, A.K., Biswas, M. and Samman, M.M. (1991). “Damage detection from changes in curvature mode shapes”, *Journal of Sound and Vibration*, 145(1991), 321–332, 1991.

Park, S., Kim, Y. B. and Stubbs, N. (2002). “Nondestructive damage detection in large structures via vibration monitoring”, *Electronic Journal of Structural Engineering 2* (2002), 59-75, 2002.

Perera, R., Huerta, C., and Orquin, J.M. (2008). "Identification of damage in RC beams using indexes based on local modal stiffness", *Construction and Building Materials*, 22(2008), 1656-1667,2008.

Pereyra, L., Osegueda, R., Carrasco, C., and Ferregut, C. (2000). “Detection of damage in a stiffened plate from fusion of modal strain energy differences”, *Proceedings of International Modal Analysis Conference (IMAC-XVIII)*, San Antonio, TX, 1556-1562, 2000.

Petro, S.H., En, S., GangaRao, S., and Venkatappa, S. (1997). “Damage detection using vibration measurement”, *Proceedings of International Modal Analysis Conference (IMAC-XV)*, Orlando, FL, 113-119, 1997.

Salawu, O.S. (1997). “Detection of structural damage through changes in frequency: A review”, *Engineering Structures*, 19(9), 718-723, 1997.

Salesh, F., Supriyadi, B., Suhendro, B. and Tran, D. (2004). “Damage detection in non-prismatic reinforced concrete beams using curvature mode shapes”, *Structural Integrity and Fracture* International Conference: *SIF2004*, 26-29 September, Brisbane, Australia, 331-337, 2004.

Sazonov, E., and Klinkhachorn, P. (2004). “Optimal spatial sampling interval for damage detection by curvature or strain energy mode shapes”, *Journal of Sound and Vibration*, 285(2005), 783-801, 2005.

Shi, Z.Y., and Law, S.S. (1998). “Structural damage localization from modal strain energy change”, *Journal of Sound and Vibration*, 218(1998), 825-844, 1998.

Shih, H. W., Thambiratnam, D. P., and Chan, T. H. T. (2009). "Vibration based structural damage detection in flexural members using multi-criteria approach", *Journal of Sound and Vibration*, 323, 645 – 661, 2009.

Stubbs, N., Kim, J. T. and Farrar, C. R. (1995). "Field verification of a non-destructive damage localization and severity estimation algorithm", *Proceedings of 13th International Modal Analysis Conference*, 210-218, 1995.

Stubbs, N., Kim, J. T. and Topole, K. (1992). "An efficient and robust algorithm for damage localization in offshore platroms", *Proceedings ASCE 10th Structures Congress*, 543-546, 1992.

The Mathworks, Inc., 2010. MATLAB® R2010b [Software], The MathWorks, Inc. 3 Apple Hill Drive Natick, MA 01760-2098

Wahalathantri B.L., Thambiratnam, D. P., Chan, T. H. T. and Fawzia, S. (2010). "An improved Modal Strain Energy method for Damage Assessment", Proceedings of the tenth international conference on computational structures technology, Paper 53, 2010.

Wahalathantri B.L., Thambiratnam, D. P., Chan, T. H. T., and Fawzia, S. (2011). "A material model for flexural crack simulation in reinforced concrete elements using ABAQUS", Proceedings of the eddBE2011 conference, Brisbane, Australia, 27-29 April 2011.

Yoo, S.H., and Kim, B.S. (2000). "Characterization of a crack in a plate using strain mode shapes", *Proceedings of International Modal Analysis Conference (IMAC-XVII)*, San Antonio, TX, 1790-1795, 2000.

Yoo, S.H., Kwak, H.K., and Kim, B.S. (1999). "Detection and location of a crack in a plate using modal analysis", Proceedings *of International Modal Analysis Conference (IMAC-XVII)*, Orlando, FL, 1902-1908, 1999.

List of Figures

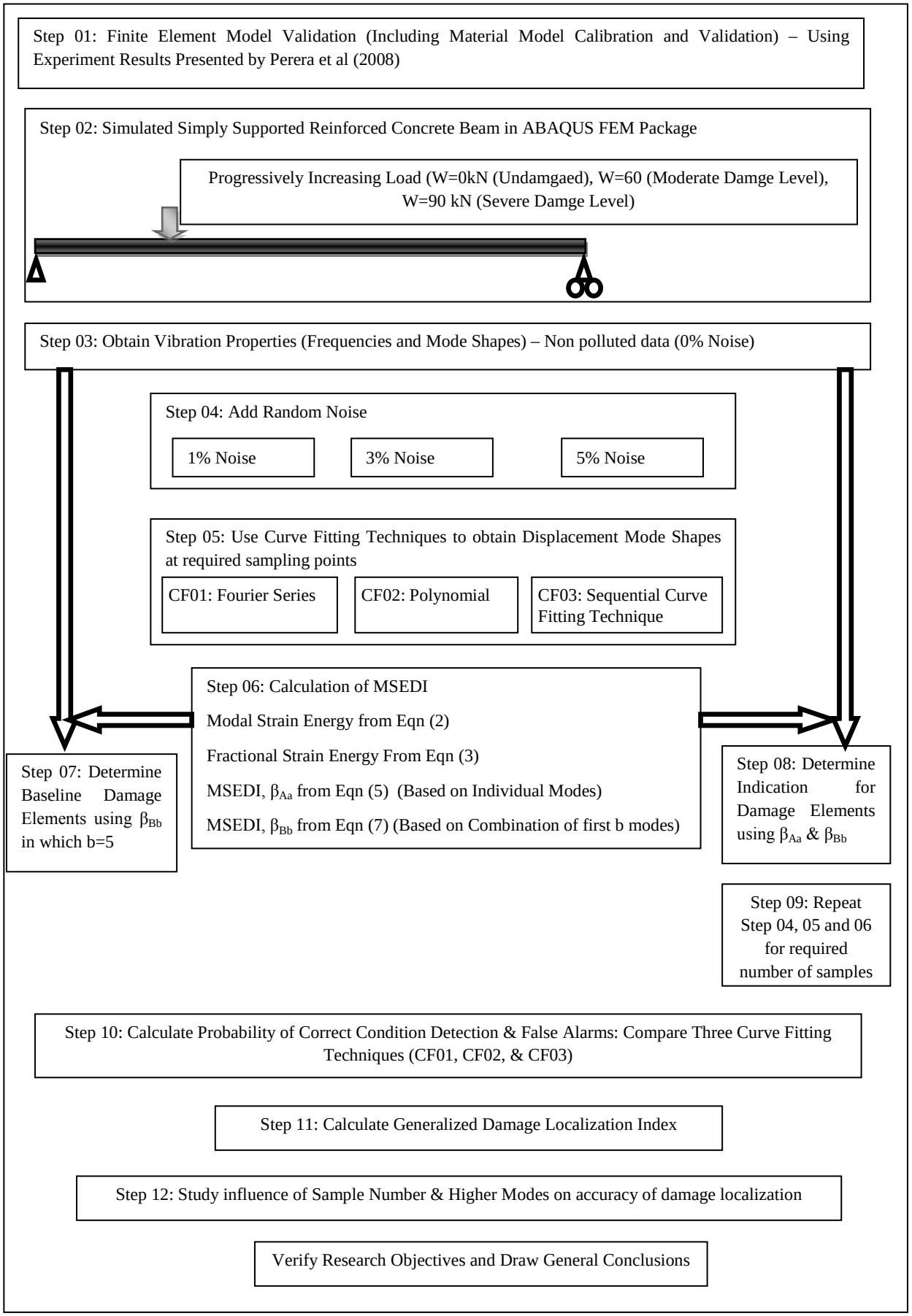

Figure 1: Methodology of the present study

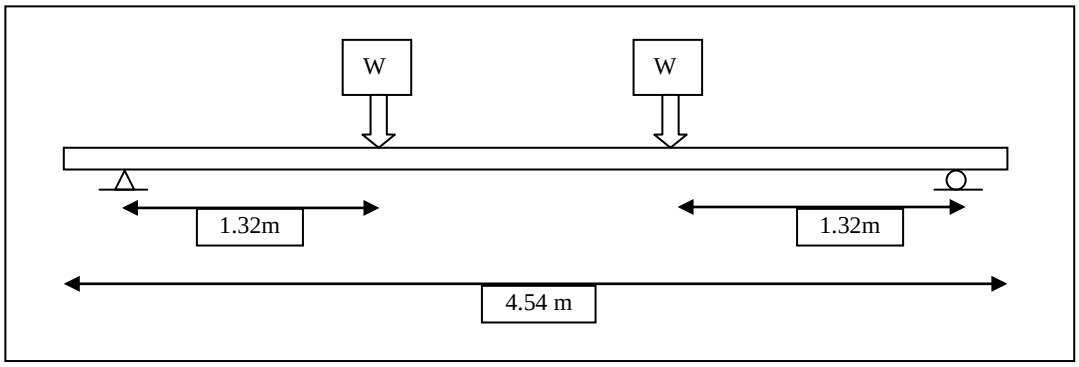

Figure 2: Four point bending setup (Perera et al (2008))

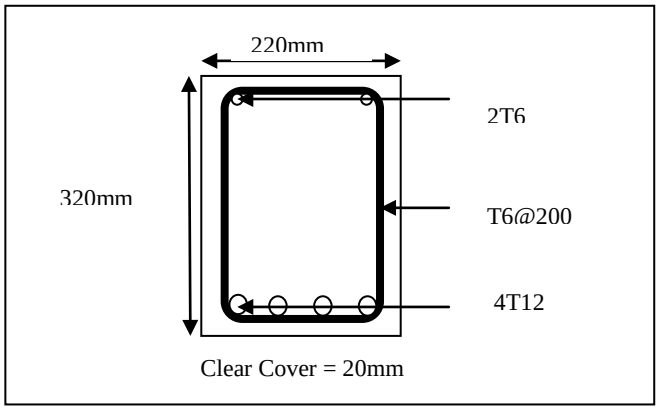

Figure 3: Cross section details of the RC beam (Perera et al (2008))

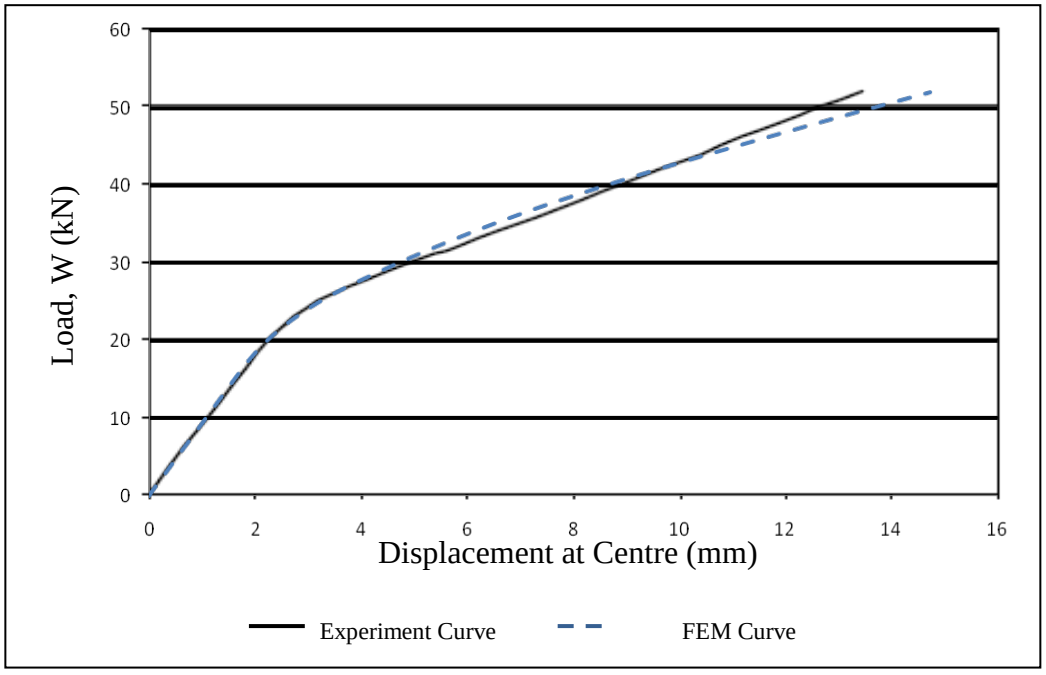

Figure 4: Load vs. mid span displacement curves (experiment (Perera et al (2008)) vs. FEM)

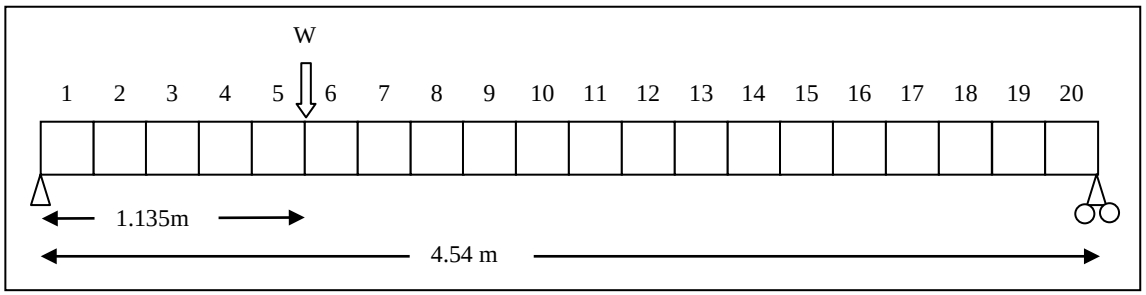

Figure 5: Loading arrangement used for the case studies

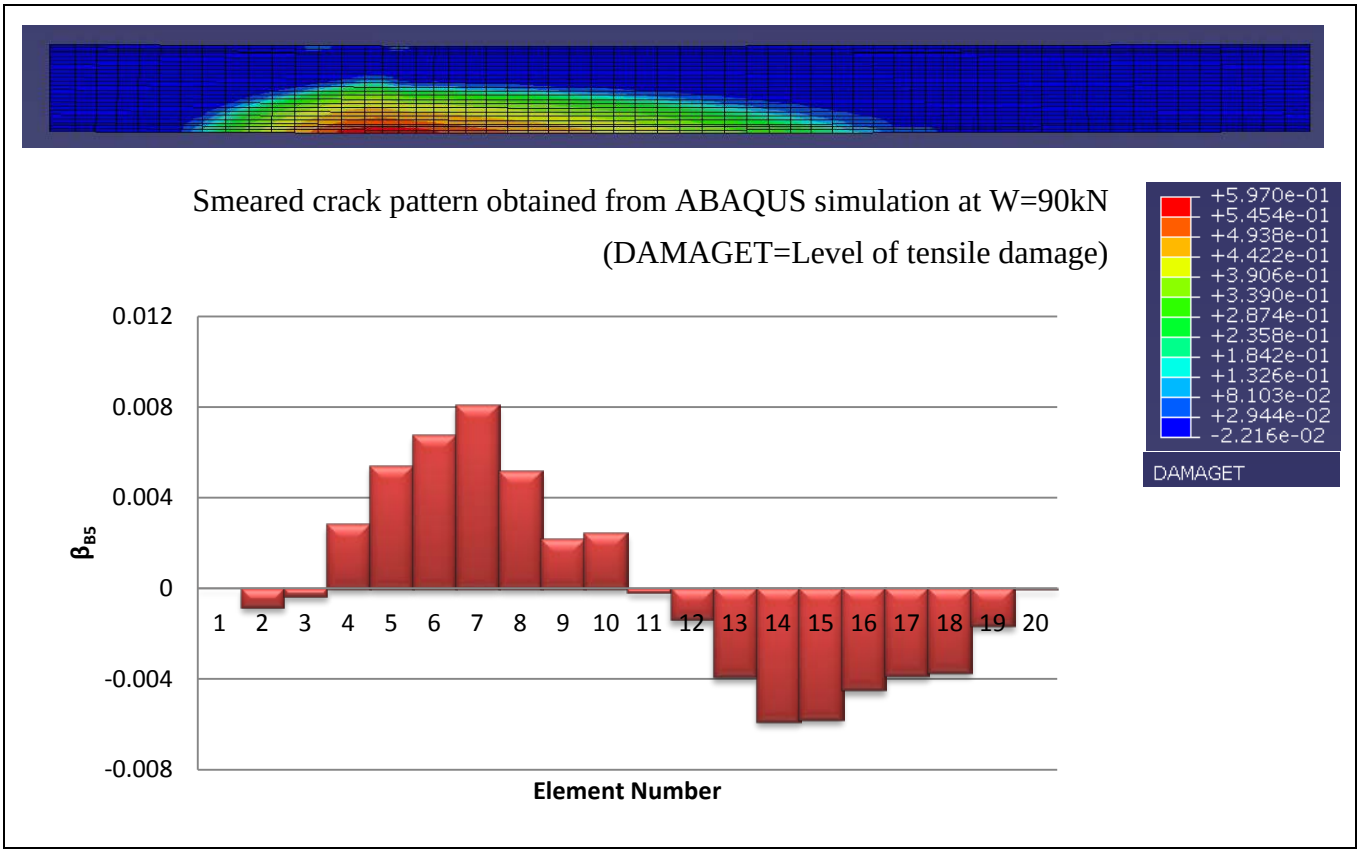

Figure 6: Variation of MSEDI along the beam without noise in mode shapes (Concentrated load of 90kN at quarter span)

CF01: Polynomial Curve Fitting Technique	CF02: Fourier Series Curve Fitting Technique	CF03: Proposed Sequential Curve Fitting Technique
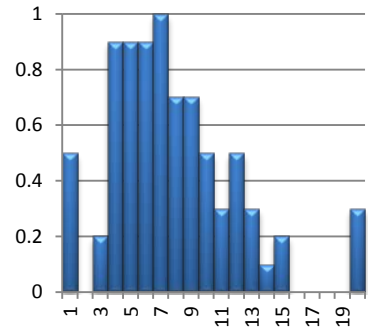 (CF01.a): Noise = 1%	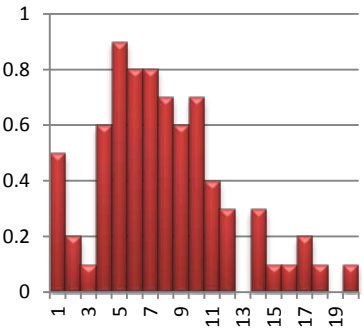 (CF02.a): Noise = 1%	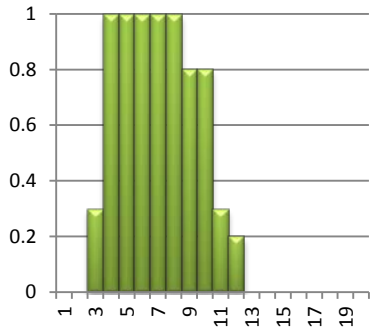 (CF03.a): Noise = 1%
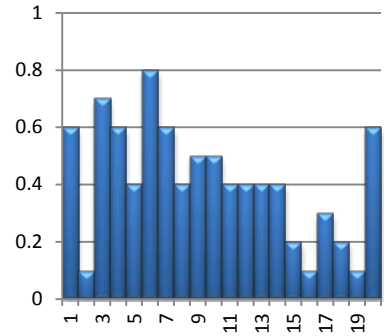 (CF01.b): Noise = 3%	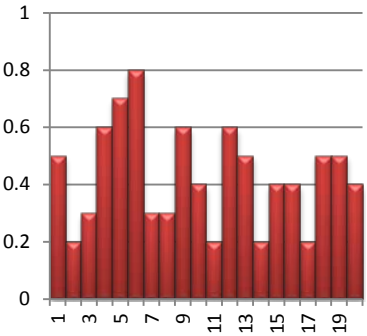 (CF02.b): Noise = 3%	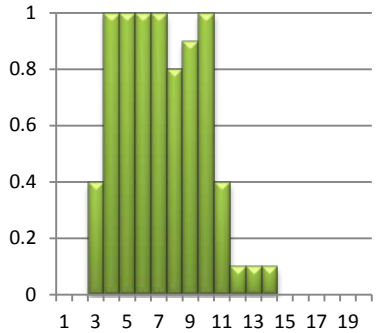 (CF03.b): Noise = 3%
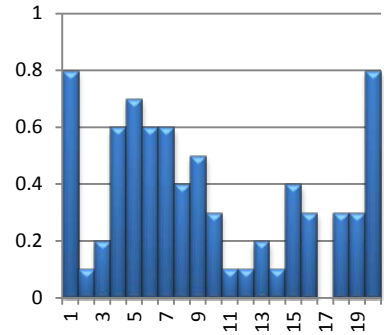 (CF01.c): Noise = 5%	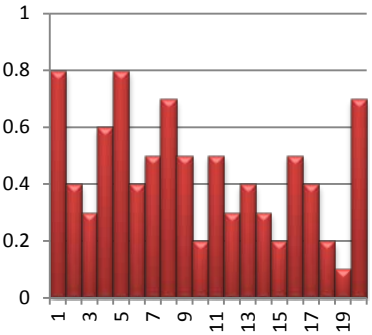 (CF02.c): Noise = 5%	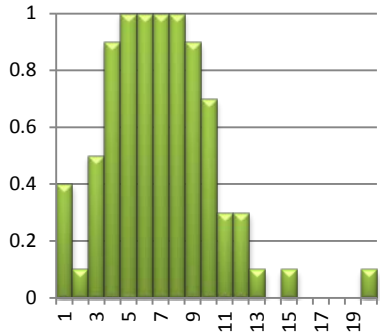 (CF03.c): Noise = 5%

Figure 7: Cumulative Probabilities of damage indication for 20 elements with three noise levels; a. 1% noise, b. 3% noise, and c. 5% noise (X-axis: Element number, Y-axis: Probabilities of damage indication using β_{B5})

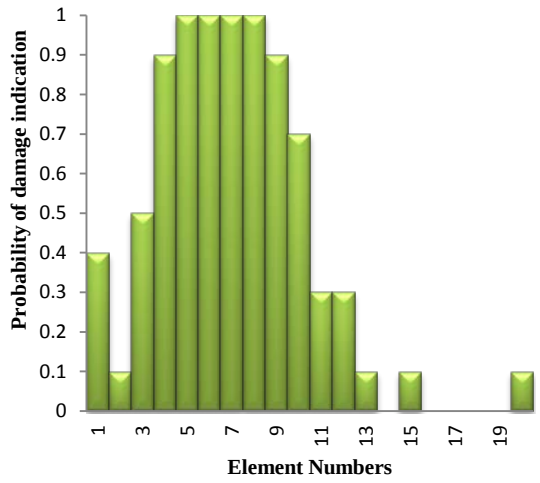

Figure 8.a: Damage detection using Probabilities obtained from β_{B5}

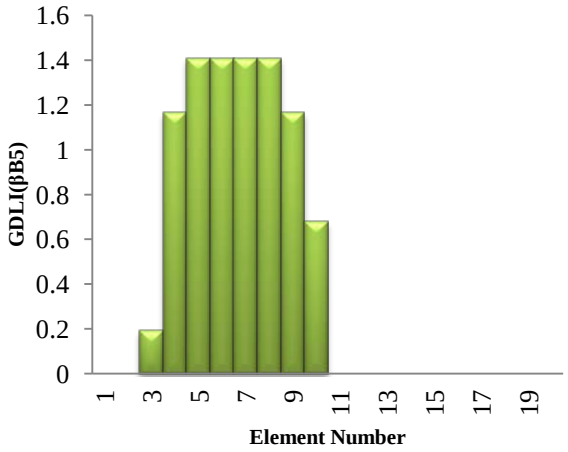

Figure 8.b: Damage detection using GDLI(β_{B5})

Figure 8: Comparison of damage detection results: (a)using probability values with β_{B5} and (b) using Generalized Damage Localization Index (GDLI(β_{B5})) – at W=90kN, 5% Noise

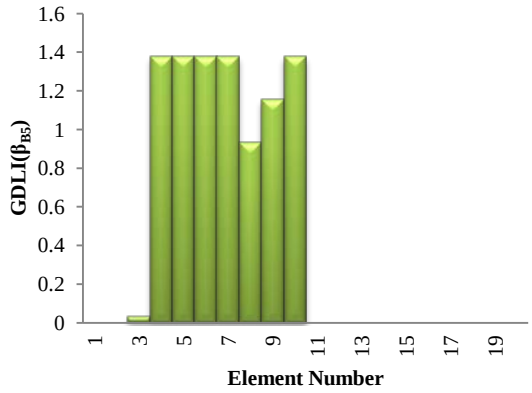

Figure 9.a: Damage detection using GDLI(β_{B5}) at 3% noise

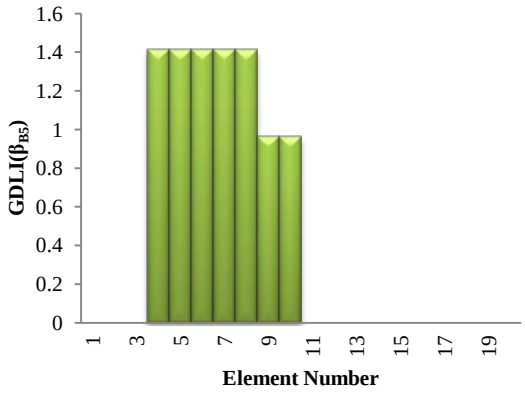

Figure 9.b: Damage detection using GDLI(β_{B5}) at 1% noise

Figure 9: Damage detection results using Generalized Damage Localization Index (GDLI(β_{B5})) – at W=90kN, a. at 3% Noise, b. at 1% Noise

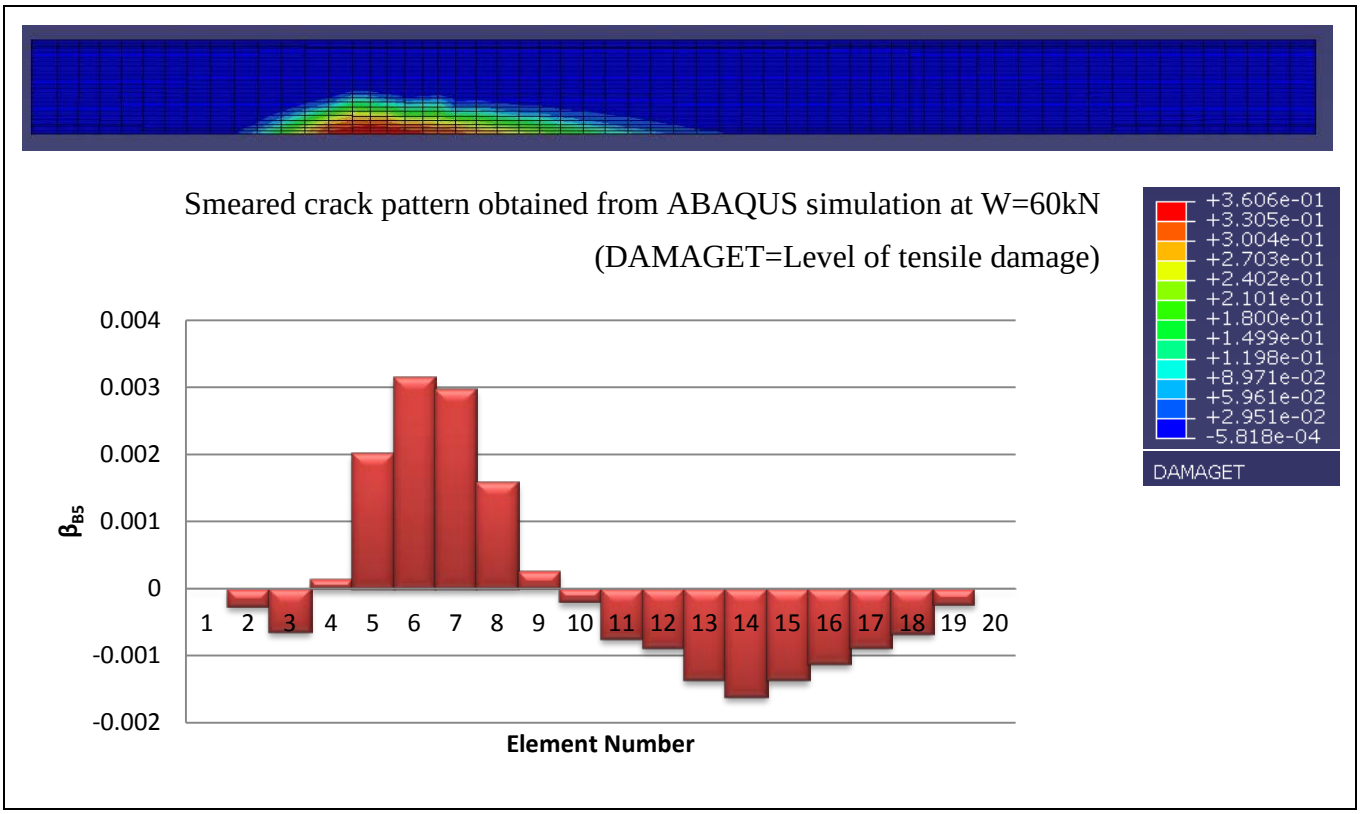

Figure 10: MSEDI variation along the beam with third curve fitting technique; without noise (Concentrated load of 60kN at quarter span)

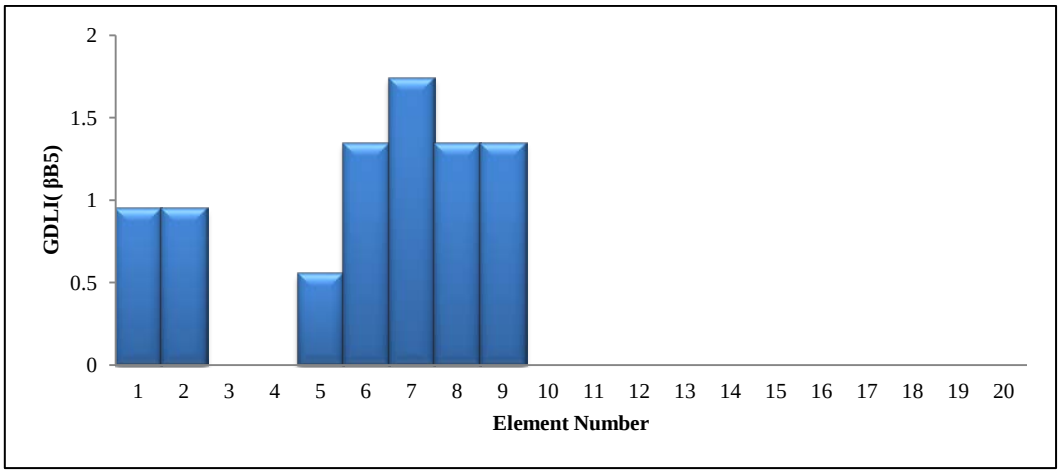

Figure 11: Damage detection using GDLI(β_{B5}) for moderate damage severity using 10 samples with 5% noise

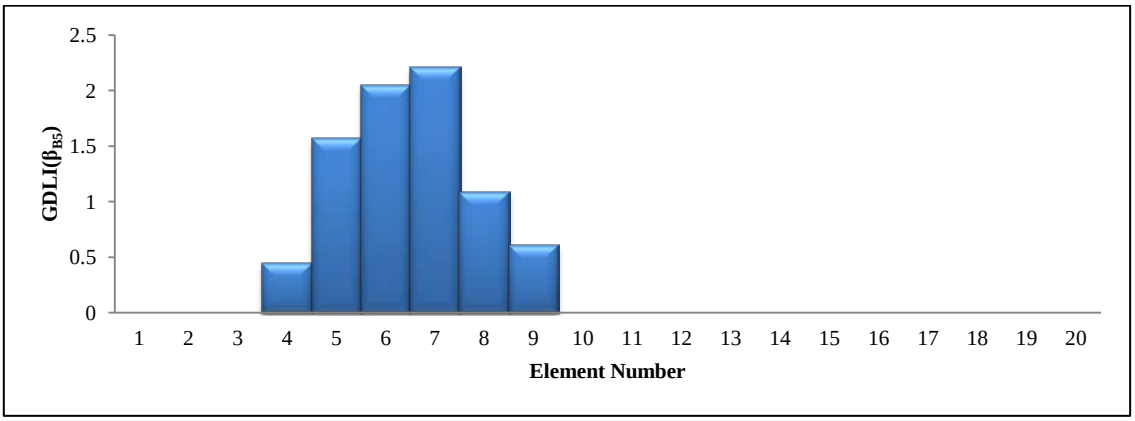

Figure 12: Damage detection using GDLI(β_{B5}) for moderate damage severity using 25 samples with 5% noise

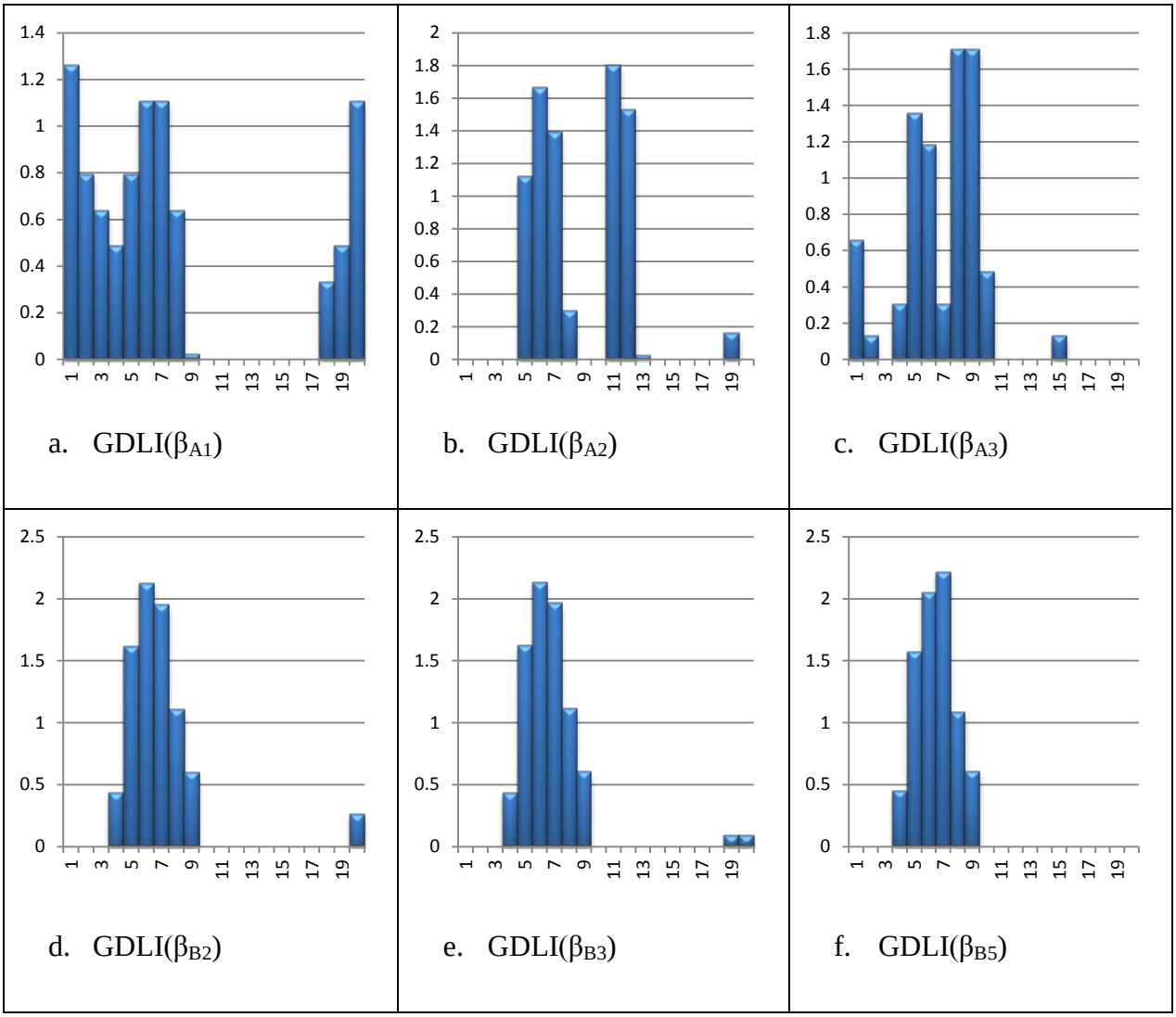

Figure 13: Damage detection of six GDLIs (a. GDLI(β_{A1}), b. GDLI(β_{A2}), c. GDLI(β_{A3}), d. GDLI (β_{B2}), e. GDLI (β_{B3}), f. GDLI (β_{B5})) using 30 samples with 5% noise at moderate damage severity (X-axis: Element number, Y-axis: Value of GDLI(β_{Aa} or β_{Bb}))

List of Tables

Table 1: Minimum number of measurement points required for Fourier series curve fitting

Order of Fourier Series	8	7	6	5	4	3	2	1
Minimum Measurement Points	17	15	13	11	9	7	5	3

Table 2: Material model data to simulate inelastic behaviour of concrete under compression

Stress (N/m^2)	Inelastic Strain (m/m)	Damage (ratio)
1.60E+07	0.00E+00	0.00E+00
2.47E+07	3.04E-04	4.43E-03
2.97E+07	7.07E-04	1.03E-02
3.16E+07	1.19E-03	1.73E-02
3.20E+07	1.70E-03	2.48E-02
2.38E+07	8.54E-03	1.24E-01
1.90E+07	1.53E-02	2.22E-01
1.62E+07	2.20E-02	3.20E-01
1.44E+07	2.86E-02	4.17E-01
1.31E+07	3.53E-02	5.13E-01
1.21E+07	4.20E-02	6.10E-01
1.13E+07	4.86E-02	7.07E-01
1.06E+07	5.52E-02	8.03E-01

Table 3: Material model data to simulate concrete behaviour under tension

Stress (N/m^2)	Inelastic Strain (m/m)	Damage (ratio)
0	0	
5880300	0	0
5145262	6.58E-05	0.05
4557232	0.000221	0.175
4542532	0.000267	0.2
4527831	0.000306	0.24
4498429	0.000462	0.375
4410225	0.000812	0.55
4351422	0.001433	0.7
4292619	0.002982	0.9

Table 4: Frequency value comparison between experiment and FEM results

Structural Arrangement	Frequency –Mode 1 Hz (% change)		Frequency –Mode 2 Hz (% change)	
	Experiment	FEM	Experiment	FEM (% Change)
1	25.32	24.715 (2.39%)	74.76	73.725 (1.38%)
2	22.03	22.208 (0.81%)	68.35	66.642 (2.50%)
3	20.50	21.024 (2.56%)	64.14	63.123 (1.59%)
4	25.32	24.715 (2.39%)	74.70	73.723 (1.31%)
5	24.47	24.708 (0.97%)	74.21	73.717 (0.66%)
6	22.94	22.493 (1.95%)	71.10	71.318 (0.31%)

Table 5: Variation of parameters A-D for three curve fitting techniques under three noise levels

Parameter		A	B	C	D
Curve Fitting Technique	Noise Level				
CF01	1%	0.825	0.738	0.175	0.262
	3%	0.658	0.525	0.342	0.475
	5%	0.700	0.475	0.300	0.525
CF02	1%	0.833	0.688	0.167	0.312
	3%	0.608	0.488	0.392	0.512
	5%	0.617	0.525	0.383	0.475
CF03	1%	0.958	0.862	0.042	0.138
	3%	0.942	0.888	0.058	0.112
	5%	0.867	0.850	0.133	0.150

Table 6: False alarms recorded at different number of samples at moderate damage severity with 5% noise

Total Number of Samples Used to Calculate Damage Index	Element Numbers with Positive False Alarms	Element Numbers with Negative False Alarms
5	1, 16, 17	-
10	1, 2	4
15	1, 2	4
20	-	4
25	-	-
30	-	-

Table 7: Minimum number of samples required at two damage severities with all three noise levels

Damage Severity	Minimum Number of Samples		
	Noise = 1%	Noise = 3%	Noise =5%
Moderate (at W=60kN)	15	20	25
Severe (at W=90kN)	5	10	15

Appendix: Notations

MSEDI = Modal Strain Energy based Damage Index

GDLI = Generalized Damage Localization Index

VBDIT = Vibration Based Damage Identification Techniques

E = Elastic Modulus

I = Second Moment of Area

i = mode number

j = node number

U_i = Modal Strain Energy of the beam for mode i

U_{ij} = Modal Strain Energy of the element j for mode i

φ_i = Mode shape values for mode i

L = Length of the beam

F_{ij} = Fractional Strain Energy of the element j for mode i

d (subscript) = Damaged state

h (subscript) = Helthy / Undamaged state

$(\beta_{ij})_1$ = Modal strain energy based damage index proposed by Stubbs et al (1992)

$(\beta_{Aa})_{ij}$ = Modal strain energy based damage index derived using mode a

$(\beta_{Ab})_j$ = Modal strain energy based damage index derived using first b modes

MF_i = Modification function for mode i (proposed by Wahalathantri et al (2010))

$[MSC]_{ij}$ = Mode shape curvature value at centre of the element j for mode i

$\left|[MSC]_{ij}\right|_{max}$ = Absolute maximum value of the mode shape curvature for mode i

MSV_i = Modal sensitivity value for mode i

λ_{id} = Eigen value of the mode i at damaged state

λ_{ih} = Eigen value of the mode i at undamaged state

CF01 = First curve fitting technique (Spline technique in MATLAB)

CF02 = Second curve fitting technique (Fourier series)

CF03 = Proposed sequential curve fitting technique

GDLI(β_{Cd}) = Generalized damage localization index derived using MSEDI, β_{Cd}

α_j = Probability of detecting j^{th} element as damaged

α_m = Mean of α_j

α_{sd} = Standard deviation of α_j

$(MS)_{jp}$ = Polluted mode shape value for node j

$(MS)_j$ = Mode shape value for node j obtained from ABAQUS simulation

Noise = percentage of noise

P_{dj} = Probability for damaged indication for element j

P_{uj} = Probability for undamaged indication for element j

P_{uuj} = Probability of correct condition detection for an undamaged element j

P_{ddj} = Probability of correct condition detection for a damaged element j

P_{udj} = Probability of false alarm for detecting damaged element j as undamaged

P_{duj} = Probability of false alarm for detecting undamaged element j as damaged

$\sum$ = sum